Chinese Chemical Letters 34 (2023) 107475

Contents lists available at ScienceDirect

Chinese Chemical Letters

journal homepage: www.elsevier.com/locate/cclet

Intercalation behavior of spiro-bipyrrolidinium cation into graphite electrodes from ethylene carbonate

Jiaxing Qi[a,b], Jichao Gao[c], Ying Wang[d], Masaki Yoshio[e], Hongyu Wang[a,b,*]

[a] State Key Laboratory of Electroanalytical Chemistry, Changchun Institute of Applied Chemistry, Chinese Academy of Sciences, Changchun 130022, China
[b] School of Applied Chemistry and Engineering, University of Science and Technology of China, Hefei 230026, China
[c] School of Chemistry and Chemical Engineering, Linyi University, Linyi 276000, China
[d] State Key Laboratory of Rare Earth Resource Utilization, Changchun Institute of Applied Chemistry, Chinese Academy of Sciences, Changchun 130022, China
[e] Advanced Research Center, Saga University, 1341 Yoga-machi, Saga 840-0047, Japan

ARTICLE INFO

Article history:
Received 18 April 2022
Accepted 26 April 2022
Available online 1 May 2022

Keywords:
Spiro-(1,1′)-bipyrrolidinium
Ethylene carbonate
Graphite intercalation compounds
Intercalated gallery height
Solvation
In situ XRD

ABSTRACT

The intercalation behavior of spiro-(1,1′)-bipyrrolidinium cation (SBP^+) into graphite electrode from spiro-(1,1′)-bipyrrolidinium tetrafluoroborate-ethylene carbonate ($SBPBF_4$-EC) solutions is investigated by conventional electrochemical tests and *in situ* X-ray diffraction measurements. Two kinds of graphite intercalation compounds (GICs) with discrete characteristic intercalated gallery heights (IGHs) (*ca.* 0.95 and 0.75 nm) can be obtained with varying the salt concentration. The effect of graphite type is also addressed.

Recently, we have proposed the application of quaternary alkyl ammonium cations (QAA^+) as the charge carries at carbon negative electrodes in the electric energy storage devices free of metals [1]. Since the risk of metal deposition at carbon negative electrodes is avoided and the thermal runaway hazard associated with the growth of metal dendrite can be completely prevented, the safety can be guaranteed. One of the key issues in these devices may be ascribed to the effective storage of QAA^+ in carbon negative electrode materials. Although we have found out that activated mesophase microbeads appears a satisfactory host material to accommodate QAA^+ [2], graphite might be a more promising candidate for this task by virtue of its low cost, environmental benignity, and abundance on the earth. Although there have been some reports on the preparation of QAA^+-graphite intercalation compounds (GICs) *via* chemical routes [3–7], it is not so easy to make good use of graphite negative electrode in QAA^+-based solutions because the influence of electrolyte solutions on its electrochemical performance has not been studied in depth. In our preliminary study [8], we have noticed that the solvent of propylene carbonate will co-intercalate into graphite electrode with a small QAA^+. Therefore, the solvation structure of QAA^+ may play a very important role in determining its storage behavior in graphite electrode.

Unfortunately, we lack convincing measures to precisely quantify the solvation number around each QAA^+ at present. However, we can flexibly tailor the solvation structure by changing the concentration of QAA^+ in a solution. In this study, we pick up spiro-(1,1′)-bipyrrolidinium tetrafluoroborate ($SBPBF_4$) as the electrolyte salt and ethylene carbonate (EC) as the solvent mainly because the concentration of $SBPBF_4$ can reach as high as 4 mol/L in EC. The intercalation behavior of SBP^+ into graphite electrode from $SBPBF_4$-EC solutions with varied concentrations is investigated by conventional electrochemical tests and *in situ* X-ray diffraction (XRD) measurements. The correlation between the electrochemical performance of graphite negative electrode and SBP^+ concentration is clarified and the effect of graphite type is addressed. The physical properties of both graphite samples are compared in Table S1 (Supporting information).

The storage behavior of SBP^+ in graphite negative electrode is mainly accessed in graphite/activated carbon (AC) capacitors. Fig. 1 depicts the separate potential profiles of graphite negative or AC positive electrodes against the *quasi*-reference electrode (QRE) in the initial galvano-static charge-discharge curves of the capacitors using $SBPBF_4$-EC solutions. The potential plateaus of graphite electrodes occupy most capacities of the cation storage, corresponding to SBP^+ intercalation into or de-intercalation from graphite electrodes. The potential plateaus of natural graphite

* Corresponding author at: State Key Laboratory of Electroanalytical Chemistry, Changchun Institute of Applied Chemistry, Chinese Academy of Sciences, Changchun 130022, China.
E-mail address: hongyuwang@ciac.ac.cn (H. Wang).

https://doi.org/10.1016/j.cclet.2022.04.073
1001-8417/

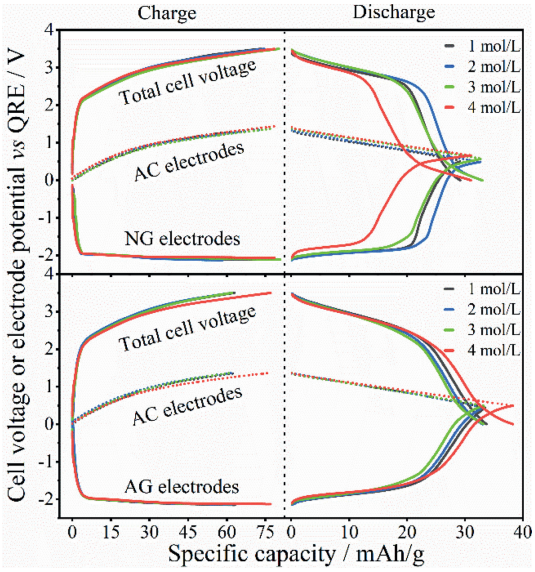

Fig. 1. Initial galvano-static charge-discharge curves of graphite/AC capacitors using 1, 2, 3 and 4 mol/L $SBPBF_4$-EC solutions and the separate potential profiles of graphite negative electrodes and AC positive electrodes against AC-QRE, respectively.

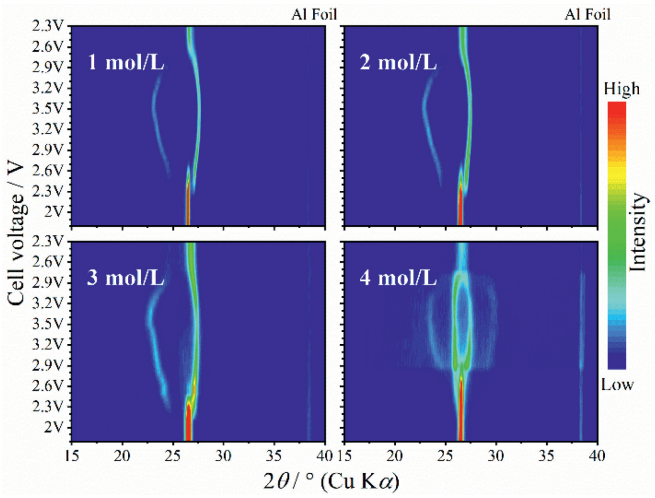

Fig. 2. *In situ* XRD patterns of NG negative electrodes in the 1, 2, 3 and 4 mol/L $SBPBF_4$-EC solutions during the initial galvano-static charge-discharge cycle of NG/AC capacitors.

(NG) electrodes become contracted with increasing of the salt concentration, especially in the case of 4 mol/L. On the other hand, the potential plateaus of the artificial graphite (AG) almost overlap with each other in all the solutions of $SBPBF_4$-EC. This dramatic contrast may hint that the storage mechanisms of SBP^+ in both graphite negative electrodes in contact with these solutions are different.

Since the potential plateaus of graphite electrodes result from the transformations of SBP^+-GICs, *in situ* XRD measurements are performed on the graphite electrodes in contact with these solutions to characterize the crystal structures of these GICs during the initial charge-discharge cycle of graphite/AC capacitors. As exhibited in Figs. 2 and 3, during the charge process with cell voltage rising, the (002) diffraction peak (26.5°) of original graphite gradually fades down. At the same time, new diffraction peaks standing for the formation of SBP^+-GICs emerge at both higher and lower Bragg angles of 26.5°. On the contrary, during the discharge with the cell voltage dropping down, the diffraction peaks of SBP^+-GICs

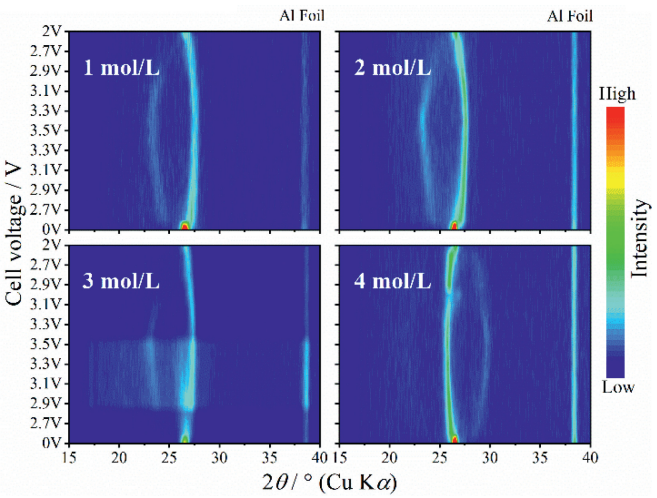

Fig. 3. *In situ* XRD patterns of AG negative electrodes in the 1, 2, 3 and 4 mol/L $SBPBF_4$-EC solutions during the initial galvano-static charge-discharge cycle of AG/AC capacitors.

gradually disappear, while the (002) peak of graphite will return. Therefore, the intercalation or de-intercalation of SBP^+ into or from graphite electrodes correspond to the charge or discharge processes of graphite/AC capacitors, respectively. For both NG and AG in the solutions of 1–3 mol/L (Figs. 2 and 3), the *in situ* XRD patterns for SBP^+-GICs generally possess a couple of peaks characteristic of the intercalated gallery heights (IGHs) near 0.952 nm. However, when the salt concentration increases to 4 mol/L, the *in situ* XRD patterns of the natural and artificial graphite electrodes are very different. There are two couples of SBP^+-GICs' peaks in the case of NG, which belong to IGHs of 0.947 and 0.742 nm, respectively. The smaller IGH value (0.742 nm) may represent the SBP^+-GICs with less EC solvents co-intercalated into graphite than those with the larger IGH values (0.947–0.952 nm). In contrast, there is only one couple of SBP^+-GICs' peaks as to AG, which corresponds to the IGH values around 0.742 nm. This unique feature means that AG is more favorable for the formation of SBP^+-GICs with milder EC co-intercalation.

From each *in situ* XRD pattern demonstrating the formation SBP^+-GICs in Figs. 2 and 3, the key parameters of IGH and stage number (SN) can be calculated according to the procedures introduced [9,10]. They are plotted against the cell voltage in Fig. 4. Both NG and AG electrodes experience the decrease of SN in the charge process but the increase of SN in the discharge process. On one hand, in the solutions of 1–3 mol/L, nearly all the IGH values fluctuate around 0.95 nm. On the other hand, when the salt concentration amounts to 4 mol/L, NG electrode can develop the SBP^+-GICs with two sets IGHs, about 0.947 and 0.742 nm, respectively. By contrast, in the case of AG, there are merely the IGH values near 0.742 nm. Why AG appears more selective than NG towards the intercalation of EC-solvated SBP^+? The previous studies have discovered that there are considerable structural defects in AG [11], which may be helpful for stripping off the surplus EC solvent bond to the cation during its intercalation into the graphite.

The cycle performance of graphite/AC capacitors using $SBPBF_4$-EC solutions is compared in Fig. 5. The capacity fades drastically in NG/AC capacitors using the 4 mol/L solution. By a big contrast, the AG/AC capacitors display very satisfactory cycle-ability, especially in the cases of highly concentrated solutions, which might be in a great part ascribed to the formations of SBP^+-GICs with neat solvation structures.

In conclusion, the intercalation of SBP^+into graphite negative electrodes from "diluted" $SBPBF_4$-EC solutions give rise to the

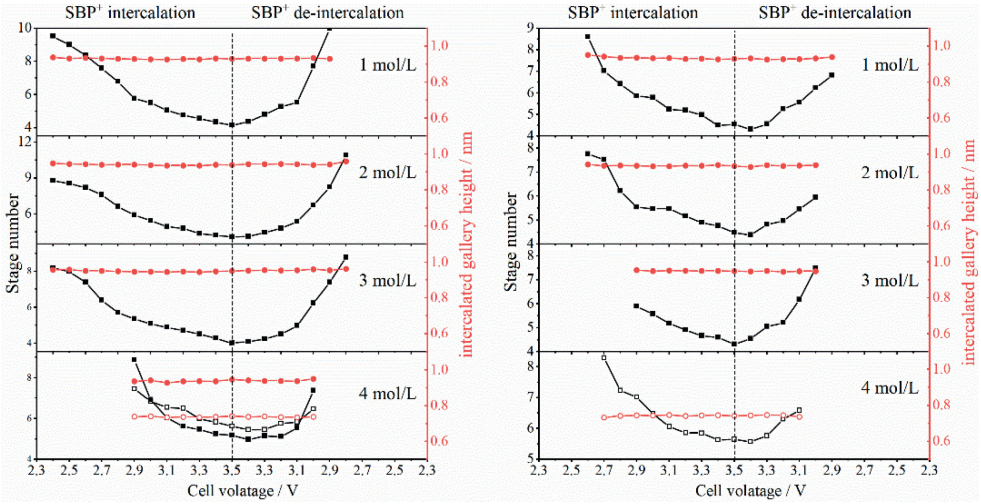

Fig. 4. Evolvements of the stage number (SN) and intercalated gallery height (IGH) of SBP^+-GICs developed in Figs. 2 and 3.

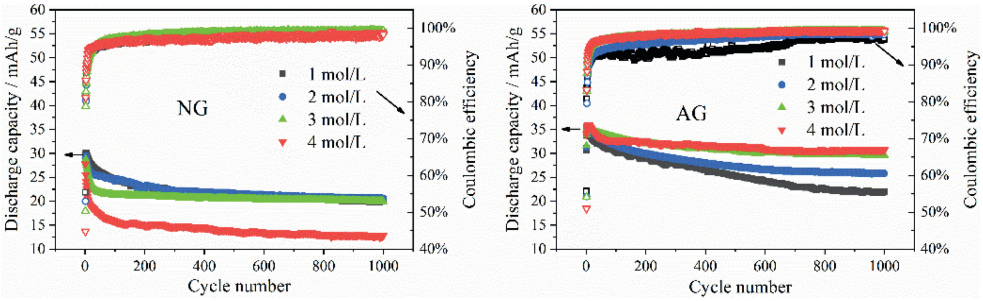

Fig. 5. Cycle performance of graphite/AC capacitors using $SBPBF_4$-EC solutions.

SBP^+-GICs with the IGH values around 0.95 nm. Once the salt concentration rises to 4 mol/L, a new kind of SBP^+-GICs with the IGH values about 0.75 nm will form, implying that less EC solvent co-intercalated into graphite electrode with SBP^+ cation. In the case of NG in the 4 mol/L solution, both kinds of SBP^+-GICs coexist. By contrast, AG negative electrode in the 4 mol/L solution only displays neat IGH values around 0.75 nm. This indicates that the abundant defects in AG help filter out SBP^+ heavily solvated by EC during its interaction into graphite.

Declaration of competing interest

All of the authors declare there is no interest conflict.

Acknowledgment

This work was financially supported by National Natural Science Foundation of China (No. 21975251).

Supplementary materials

Supplementary material associated with this article can be found, in the online version, at doi:10.1016/j.cclet.2022.04.073.

References

[1] C. Zheng, M. Yoshio, L. Qi, H. Wang, J. Power Sources 260 (2014) 19–26.
[2] J. Li, C. Zheng, L. Qi, H. Wang, Electrochim. Acta 283 (2018) 1712–1718.
[3] W. Sirisaksoontorn, A.A. Adenuga, V.T. Remcho, M.M. Lerner, J. Am. Chem. Soc. 133 (2011) 12436–12438.
[4] W. Sirisaksoontorn, M.M. Lerner, Inorg. Chem. 52 (2013) 7139–7144.
[5] W. Sirisaksoontorn, M.M. Lerner, Carbon 69 (2014) 582–587.
[6] K. Gotoh, C. Sugimoto, R. Morita, et al., J. Phys. Chem. C 119 (2015) 11763–11770.
[7] H. Zhang, Y. Wu, W. Sirisaksoontorn, V.T. Remcho, M.M. Lerner, Chem. Mater. 28 (2016) 969–974.
[8] J. Li, Y. Huang, H. Wang, J. Electrochem. Soc. 165 (2018) A4012–A4017.
[9] X. Zhang, N. Sukpirom, M.M. Lerner, Mater. Res. Bull. 34 (1999) 363–372.
[10] M.S. Dresselhaus, G. Dresselhaus, Adv. Phys. 51 (2002) 1–186.
[11] J. Li, X. Wang, Y. Wang, et al., J. Electrochem. Soc. 166 (2019) A2349–A2356.